A ubiquitinome analysis to study the functional roles of the proteasome associated deubiquitinating enzymes USP14 and UCH37

Lennart van der Wal, Karel Bezstarosti, Jeroen A.A. Demmers [*]

Proteomics Center, Erasmus University Medical Center, Rotterdam, the Netherlands

ABSTRACT

The removal of (poly)ubiquitin chains at the proteasome is a key step in the protein degradation pathway that determines which proteins are degraded and ultimately decides cell fate. Three different deubiquitinating enzymes (DUBs) are associated to the human proteasome, PSMD14 (RPN11), USP14 and UCH37 (UCHL5). However, the functional roles and specificities of these proteasomal DUBs remain elusive. To reveal the specificities of proteasome associated DUBs, we used SILAC based quantitative ubiquitinomics to study the effects of CRISPR-Cas9 based knockout of each of these DUBs on the dynamic cellular ubiquitinome. We observed distinct effects on the global ubiquitinome upon removal of either USP14 or UCH37, while the simultaneous removal of both DUBs suggested less functional redundancy than previously anticipated. We also investigated whether the small molecule inhibitor b-AP15 has the potential to specifically target USP14 and UCH37 by comparing treatment of wild-type versus USP14/UCH37 double-knockout cells with this drug. Strikingly, broad and severe off-target effects were observed, questioning the alleged specificity of this inhibitor. In conclusion, this work presents novel insights into the function of proteasome associated DUBs and illustrates the power of in-depth ubiquitinomics for screening the activity of DUBs and of DUB modulating compounds.

Significance: Introduction: The removal of (poly)ubiquitin chains at the proteasome is a key step in the protein degradation pathway that determines which proteins are degraded and ultimately decides cell fate. Three different deubiquitinating enzymes (DUBs) are associated to the human proteasome, PSMD14/RPN11, USP14 and UCH37/UCHL5. However, the functional roles and specificities of these proteasomal DUBs remains elusive. Materials & Methods: We have applied a SILAC based quantitative ubiquitinomics to study the effects of CRISPR-Cas9 based knockout of each of these DUBs on the dynamic cellular ubiquitinome. Also, we have studied the function of the small molecule inhibitor b-AP15, which has the potential to specifically target USP14 and UCH37. Results: We report distinct effects on the ubiquitinome and the ability of the proteasome to clear proteins upon removal of either USP14 or UCH37, while the simultaneous removal of both DUBs suggests less redundancy than previously anticipated. In addition, broad and severe off-target effects were observed for b-AP15, questioning the alleged specificity of this inhibitor. Conclusions: This work presents novel insights into the function of proteasome associated DUBs and illustrates the power of in-depth ubiquitinomics for screening the activity of DUBs and of DUB modulating compounds.

1. Introduction

The ubiquitin-proteasome system (UPS) plays an important role in the maintenance of cellular proteostasis. Protein degradation by the UPS clears the cell of misfolded, damaged and unneeded proteins. When proteins are degraded via the UPS, the 8.5 kD protein ubiquitin (or polymeric versions hereof) is conjugated to the target protein as a posttranslational protein modification, after which the protein is sent to the 26S proteasome and degraded into peptides, thus abolishing target protein activity [1,2]. Malfunctioning of the UPS has been shown to play a role in neurodevelopmental disorders [3] and cancer [4,5]. Drugs that inhibit proteasome activity, such as Bortezomib and Carfilzomib, are used in the clinic to treat hematologic cancers such as multiple myeloma [6]. Although these approaches have proven to be useful, they suffer from induced resistance of cancer cells to such small molecule compounds [6,7]. In contrast, in neurodegenerative disorders where protein aggregation impairs cellular functions, activation of the proteasome appears to be beneficial [8,9].

The signaling event that acts as the trigger for subsequent actions in UPS mediated protein degradation is the conjugation of ubiquitin to the ε-amino group of a lysine residue in the target protein. This protein modification involves a signaling cascade, in which the E3 ligase conjugates the ubiquitin C-terminal carboxyl group to the target lysine in the final step [10,11]. Ubiquitin itself can also be modified by other ubiquitin moieties at one of its seven lysine residues or at the N-terminal methionine, which can lead to complex branched polyubiquitin structures [4,11–13]. It is generally assumed that these different polyubiquitin structures play roles in signaling events in the cell [4]. For instance, K48 linked polyubiquitin is thought to mark a protein for degradation via the proteasome, whereas K63 linked polyubiquitin has, in addition to proteasome mediated degradation, also been associated to autophagy [4,10]. However, the functional roles of these different polyubiquitin structures are still not well understood. The recent discovery of mixed linkage or heterotypic polyubiquitin chains has even expanded the repertoire of ubiquitin conjugates with yet unknown roles [11,14]. Ubiquitin can also be modified by other posttranslational modifications (PTMs), such as phosphorylation and acetylation to modulate polyubiquitin functions [12] One notable example is the PINK1 dependent phosphorylation of S65 of ubiquitin [15,16].

Most proteasomes consist of the 20S proteasome, or core particle (CP), and one or two 19S proteasomes or regulatory particles (RP or caps) [17]. Although the proteolytic activity of the proteasome is located inside the 20S subunit, the association with a cap is necessary for the guidance of a protein into the proteasome barrel. The exact composition of the 20S proteasome itself may vary. For instance, in the immunoproteasome the constitutive subunits β1, β2 and β5 have been replaced by counterparts with altered peptide-cleavage properties to turn it into a specialized CP, enabling more efficient antigen processing for presentation on MHC class I molecules [18]. Several different cap structures have been identified, such as the ATP-dependent 19S cap and the ATP-independent S11 and PA200. The superstructure of one or two 19S and the 20S proteasomes is defined as the 26S proteasome and is the most abundant and well known proteasome structure for the degradation of ubiquitinated proteins [19,20]. The 19S proteasome recognizes ubiquitinated proteins by means of its ubiquitin receptors RPN10 and RPN13, which then allows the 20S proteasome to degrade ubiquitinated proteins in an ATP-dependent manner [21,22]. In addition, this association of one or two 19S particles to a 20S proteasome induces conformational changes in the latter, which results in stimulation of protein degradation [21].

Prior to protein degradation, the (poly)ubiquitin chain is first removed by one of the proteasome associated deubiquitinating enzymes (DUBs). Three proteasome associated DUBs have been identified in mammals: PSMD14 (also known as POH1 or RPN11), USP14 (or UBP6) and UCH37 (or UCHL5) [23]. They belong to different deubiquitinase families and show distinct differences in their function and mode of action [23]. PSMD14 belongs to the JAMM (JAB1/MPN/MOV34 metalloenzyme domain) family of DUBs and is well conserved throughout evolution. Of the three proteasomal DUBs, PSMD14 is the only essential one in *Saccharomyces cerevisiae* and mammals, both in terms of deubiquitinating activity and its stabilizing role in the proteasome structure [24–27]. In contrast to higher eukaryotes, *S. cerevisiae* is able to survive with an inactive mutant of PSMD14, provided that the yeast USP14 analog UBP6 is still present and active [26]. Furthermore, PSMD14 has been reported to play a role in several key cell processes such as DNA repair [28] and maintenance of pluripotency [29].

USP14 is an evolutionary conserved cysteine protease that belongs to the ubiquitin-specific protease (UBP) subfamily and is the sole proteasomal DUB that is a non-stoichiometric subunit of the proteasome, as only 30–40% of all proteasomes carry the USP14 subunit [30,31]. Not only are mammalian cells and yeast viable without USP14 [26,30], proteasomes lacking USP14 display a higher protein degradation rate [30] than wild-type proteasomes, suggesting a regulatory role in rescuing proteins from degradation by deubiquitination. We have recently shown by immunopurification experiments in *Drosophila* that the association of USP14 to the 20S proteasome is weaker than that of other associated subunits [32]. Extra-proteasomal functions of USP14 have been described, such as in Wnt signaling by deubiquitination of Disheveled [33] and arguably in Hedgehog signaling by the deubiquitination of Kif7 [34].

UCH37 (or UCHL5) belongs to the UCH subfamily of cysteine protease DUBs and is not essential for basal proteasome functioning [35]. UCH37 binds to the deubiquitinase adaptor domain (DEUBAD) of ADRM1/RPN13 [35–37]. Furthermore, UCH37 is a constituent of the chromatin remodeling complex INO80 [35,37].

Several mechanistic studies have revealed differences in the mechanisms by which the various proteasomal DUBs remove (poly)ubiquitin from their substrates. PSMD14 can only remove polyubiquitin *en bloc*, because of the physical constraints of the proteasomal structure [10,38]. USP14 removes ubiquitin *en bloc* [39] or cleaves ubiquitin from the distal end of a Lys48-linked polyubiquitin chain, as suggested by in vitro experiments [40]. UCH37 has been shown to catalyze the removal of single ubiquitin moieties [23], although at a much lower rate than USP14. This suggests that it may hardly occur in vivo, where the loss of USP14 induces a decrease in the free ubiquitin pool [23,41]. Recently, it was found that UCH37 exclusively cleaves branched chains bearing K48 linkages and that loss of UCH37 activity on the proteasome impedes the degradation of proteins modified with branched chains [42].

In recent years, there have been advances in the large-scale analysis of protein ubiquitination, in particular by mass spectrometry based approaches [43]. Tryptic digestion of ubiquitinated protein substrates results in the generation of peptides carrying a diglycine (diGly) remnant at the target lysine residue, which can be efficiently immunopurified. Quantitative mass spectrometry assays such as SILAC or isobaric labeling then allow for the analysis of thousands of ubiquitination sites simultaneously. Despite some mechanistic knowledge, the target specificities of the different proteasomal DUBs remain elusive. In vitro studies have shown that USP14 and UCH37 have a broad ubiquitin chain recognition specificity [23], but their protein target specificities have yet to be demonstrated. Here, we apply in-depth mass spectrometry based quantitative ubiquitinomics to investigate the cellular roles of the proteasome associated DUBs USP14, UCH37 and PSMD14. We hypothesize that the dynamics of the cellular ubiquitinome and proteome upon modulation of proteasomal DUB abundance levels may reveal their respective cellular functions. In addition, we apply this methodology to small molecule inhibitors that allegedly target specific proteasome associated DUBs.

2. Experimental methods

2.1. Cell culturing

Human cervical cancer cells (HeLa) were grown in Dulbecco's Minimal Eagle Medium (DMEM) supplemented with 10% fetal bovine serum (FBS, heat inactivated; Gibco) and 100 units/mL penicillin/streptomycin. For SILAC experiments, cells were cultured in specially formulated DMEM (Thermo) lacking conventional Arginine and Lysine, supplemented with 10% dialyzed FBS (Sigma), 100 units/mL penicillin/streptomycin and glutamax (Gibco). SILAC cells were grown in medium containing either conventional lysine and arginine (Sigma; referred to as 'Light') or lysine-8 ($^{13}C_6$ and $^{15}N_2$) and arginine-10 ($^{13}C_6$ and $^{15}N_4$) (Cambridge Isotope Laboratories; referred to as 'Heavy'). Cells were grown in this medium for at least 6 doublings before further treatment. Incorporation of the heavy isotope labels was verified by mass spectrometry. For the b-AP15 treatment, cells were treated with 1 μM b-AP15 (UBPbio, F2101) or an equivalent volume of DMSO for 8 h, after which the cells were harvested.

Harvesting of cells was performed as described earlier [44]. Briefly, cells were dissociated with trypsin-EDTA, pelleted and washed thrice in PBS. Lysis was performed using Phase Transfer Surfactant (composed of

100 mM Tris-HCl (pH 8.5), 12 mM sodium deoxycholate and 12 mM sodium N-lauroylsarcosinate [45], then boiled briefly and sonicated using a Bioruptor (Diagenode) for 10 min.

For immunofluorescence, cells were stained using Phalloidin (Life Technologies) and DAPI-containing mounting medium (Vectashield) according to the manufacturer's instructions.

Stable knockdown cell lines were generated using lentiviral transduction, followed by puromycin selection for at least 2 weeks. In brief, plasmids containing shRNA targeting either USP14, UCH37 or PSMD14 in a p.LKO.1 backbone were obtained using an in-house service. Lentiviral particles were generated in 293 T cells using a 2nd generation lentiviral system [46] by using PEI to transfect in the packaging, envelope and targeting plasmids. Lentiviral particles were collected by aspirating medium from lentiviral producing cells. Lentivirus containing medium was incubated on cells for 24 h, after which the cells were allowed to recover before puromycin selection was started for at least 2 weeks. In order to generate double knockdown cell lines, lentiviral particles with neomycin resistance were generated to allow for a selection step.

Full knockout cell lines were generated using CRISPR-Cas9 [47]. In brief, sgRNA targeting either USP14, UCH37 or PSMD14 was cloned into a pspCas9 plasmid. Different permutations of 2 sgRNA plasmids were used to target proteins using a single nicking (D10A) Cas9 to allow for heightened specificity. After transduction of Cas9 plasmids with sgRNA, single cells were seeded in order to obtain a monoclonal population. Putative candidates were selected using PCR of the nick-sites. Knockout was confirmed by immunoblotting and targeted mass spectrometry.

2.2. Proteasome immunoprecipitation

Purification of 26S proteasomes was performed using a commercial purification kit (UBPBio, #J4320) as described by the manufacturer. Ten mg total protein was used as the input per sample. Upon purification, samples were spun down before further preparation for mass spectrometry. According to the manufacturer's instructions, a control pulldown was performed using GST instead of GST-Ubl to be able to correct for background binding.

2.3. Glycerol gradient

Protein complex size analysis using glycerol gradients was performed as described earlier [32]. Briefly, gradients were prepared from 5 to 30% glycerol in polyallomer tubes (331,374, Beckmann) using a gradient master (Biocomp, settings Time 2:13, angle 81.5, velocity 16). Non-denatured cell lysates (lysis buffer: 50 mM HEPES-KOH pH 7.6, 100 mM KCl, 0.1%NP40, protease inhibitors) were carefully layered onto the gradients and centrifuged for 17 h at 4 °C at 32 krpm. Next, 24 fractions of 560 μl each were harvested, aliquoted and stored at −80 °C until further use. Adjacent fractions (3 and 4, 5 and 6, etc.) were pooled so that 13 samples were obtained. These samples were analyzed using SDS-PAGE analysis.

2.4. Antibodies

Lysates were diluted into 4× Laemmli buffer, boiled and sonicated for 5 min. Lysates were then separated on a 10% or 12% SDS-PAGE polyacrylamide gel and transferred to a 0.2 μm PVDF membrane (Merck Milipore). Membranes were blocked in 5% skim milk in PBS with 0.1% Tween for 1 h, incubated overnight for primary antibodies and incubated for 1.5 h for the secondary antibody. Bands were visualized using ECL imaging on an Amersham Imager. The primary antibodies used were: Rabbit-α-USP14 (Bethyl, # A300-919A, 1:1000), Rabbit-α-USP14 (Abcam, EPR15943, 1:4000), rabbit-α-UCH37 (abcam, EPR4896, 1:2000), Rabbit-α-PSMD14 (Abcam, EPR4257, 1:2000), Mouse-α-α Tubulin (Sigma, 1:5000), Mouse-α-GAPDH (Abcam, Ab8245, 1:5000), Mouse-α-ubiquitin (P4D1, CST, #3936, 1:1000), Rabbit-

α-ubiquitin (SPA-200, Enzo, 1:1000), Rabbit-α-PSMA5 (CST, #2457, 1:5000), Rabbit-α-PSMB5 (CST, #12919, 1:1000), Rabbit-α-RAD18 (CST, #9040, 1:1000), Rabbit-α-SQSTM1 (CST, #8025, 1:1000), Rabbit-α-PLXND1 (CST, #92470, 1:1000) and Rabbit-α-CAV1 (CST, #3238, 1:1000). The secondary antibodies used were HRP-Goat-α-Rabbit (Sigma, #12–348, 1:5000) and HRP-Goat-α-Mouse (Sigma, #12–349, 1:5000).

2.5. Survival assay

Treatment of HeLa wild-type (WT) and KO cells with Tunicamycin (Sigma, T7765), Bortezomib (UBPbio, F1201), b-AP15 (UBPbio, F2101) or 1,4-Dithiothreitol (DTT, Sigma, D9779) was performed for 8 h (Bortezomib and b-AP15) or 24 h (Tunicamycin and DTT), after which the cells were allowed to recuperate for 24 h. Cells were then fixed using an acetic acid: methanol (1:3, *v/v*) solution for 5 min and stained using 0.5% crystal violet in a methanol: water (1:4, v/v) solution for 30 min.

2.6. Mass spectrometry

Analysis of the global proteome and enrichment for diGlycine (diGly) remnant containing peptides using antibody based enrichment was performed as described before [44]. Briefly, proteolytic peptides were fractionationed using high pH reverse-phase (RP) chromatography. For the RP chromatography, a protein digest: stationary phase ratio of 1: 50 was used and peptides were eluted in three fractions using increasing amounts of acetonitrile (7%, 13.5% and 50%). Fractions and flow-through were subsequently dried to completeness by lyophilization. For immunoprecipitation of diGly peptides, ubiquitin remnant motif (K-ε-GG) antibodies coupled to beads (PTMscan, product #5562, Cell Signaling Technologies) were used. After immunoprecipitation, the supernatant was stored for further global proteome analysis.

Mass spectra were acquired on an Orbitrap Tribrid Lumos mass spectrometer (ThermoFisher Scientific) coupled to an EASY-nLC 1200 system (Thermo) and operating in positive mode (Tune version 3.3). Peptide mixtures were trapped on a 2 cm × 100 μm Pepmap C18 column (ThermoFisher Scientific, #164564) and separated on an in-house packed 50 cm × 75 μm capillary column with 1.9 μm Reprosil-Pur C18 beads (Dr. Maisch) at a flow rate of 250 nL/min on an EASY-nLC 1200 (ThermoFisher Scientific), using a linear gradient of 0–32% acetonitrile (in 0.1% formic acid) during 60 or 90 min. The eluate was directly sprayed into the mass spectrometer by means of electrospray ionization (ESI). For global data dependent acquisition (DDA) proteomics, full MS1 scans were recorded in the range of 375–1400 m/z at 120,000 resolution. Fragmentation of peptides with charges 2–5 was performed using HCD. The collision energy was set at 30% and previously fragmented peptides were excluded for 60 s. The resolution of tandem mass spectra (MS2) was set at 30,000 and automatic gain control (AGC) was set to 5E4 and the maximum injection time (IT) was set to 50 ms. MS2 spectra were recorded in centroid mode. The sequence of sampling was blanks first and then in order of increasing peptide input amounts to avoid any contamination of previous samples.

The relative abundances of a subset of specific proteins in the KO cells were measured using a label free targeted proteomics approach, essentially as described in [48]. Briefly, a parallel reaction monitoring (PRM) regime was used to select for a set of previously selected peptides on an Orbitrap Tribrid Lumos mass spectrometer (ThermoFisher Scientific) coupled to an EASY-nLC 1200 system (Thermo) and operating in positive mode (Tune version 3.3). Precursors were selected in the quadrupole with an isolation width of 0.7 m/z and fragmented with HCD using 30% collision energy (CE). MS2 spectra were recorded in profile mode in the Orbitrap at 30,000 resolution. The maximum injection time was set to dynamic with a minimum of 9 points measured across the chromatographic peak. See Table S11 for the m/z isolation list.

2.7. Bioinformatic analysis

Analysis of raw mass spectrometry data was performed using Max-Quant (v 1.5.6.4) [49] for DDA data and Skyline [50] for PRM data. Downstream analysis was performed using Perseus (v 1.6.1.1) and in-house software packages. Volcano plots were based on one sample *t*-tests and a 1.5-fold change was chosen as the threshold for up- or downregulation, unless stated otherwise. The settings in MaxQuant were chosen as described earlier [44]. For the LFQ analysis of the proteasome pulldown assay, an imputation step was included to cope with missing values, using a normal distribution with standard settings (i.e., width 0.3, downshift 1.8).

Functional enrichment analysis was performed using GOrilla [51,52]. A *p*-value threshold of 1E-6 was set as a cutoff for the ubiquitinated peptides. For the generation of a background list, all identified proteins in the global proteome analysis described in this paper were taken. Amino acid sequence logos were created using the web service Icelogo [53]. Dependency analysis was performed using DepMap [54,55].

3. Results

The 26S proteasome contains three associated proteins with deubiquitinating enzymes (DUB) activity, i.e. USP14, UCH37 and PSMD14, but it remains enigmatic why multiple subunits with DUB activity are needed for proper functioning. We hypothesize that if there are functional differences between these DUBs, their inactivation would affect the global cellular proteome and ubiquitinome. In order to determine the functional roles of these proteasomal DUBs, we generated cell lines in which partial or complete removal of these DUBs was established in order to compare their ubiquitinome and proteome profiles to those of wild-type (WT) cells. Partial knockdown (KD) was achieved using lentiviral transduction of shRNA, leading to a reduction of expression to about 10–20% of the WT expression levels as estimated by immunoblotting (Fig. 1B). Knockout (KO) cell lines for USP14, UCH37 and PSMD14 were generated using CRISPR-Cas9 to remove several exons from the gene by using two or three different guide RNAs simultaneously [47] (Fig. S1). At least 30% of the target protein sequences were removed from the genome this way, thus abrogating expression of the full-length protein. Immunoblotting showed that this strategy was successful in abolishing expression of the full-length protein (Fig. 1C). For confirmation, parallel reaction monitoring (PRM) targeted mass spectrometry was applied to verify the complete loss of expression of the target proteins (Fig. 1D, Fig. S2). The abundances of at least three tryptic peptides for each target protein were measured in extracts of cells in which the target proteins were knocked out.

It has been suggested that USP14 and UCH37 display DUB activity at a similar step in the protein degradation process [23], leaving the possibility that they perform redundant roles. Therefore, we also generated both a double KD and a double KO (termed 'dKD' and 'dKO', respectively) cell line in order to study this putative redundancy. This was achieved by performing another round of lentiviral transduction or CRISPR-Cas9, the efficiency of which was verified using immunoblotting and quantitative mass spectrometry (Figs. 1B–D and Fig. S2). Interestingly, while the expression levels of the 20S proteasomal subunits PSMA5 and PSMB5 were slightly reduced in dKD (Fig. 1B) or similar in dKO (Fig. 1C), the level of PSMD14 was reduced to a higher extent in these cell lines. Also, immunopurified proteasomes from dKO cells show a slight reduction in 19S constituents with respect to 20S proteasome constituents in comparison to WT cells (Fig. 2E; vide infra). This may suggest that overall levels of the 19S proteasome in the dKD and dKO cell lines may be somewhat reduced with respect to 20S proteasome levels.

Next, we attempted to knock down PSMD14 in WT cell lines using lentiviral transduction (Fig. 1A). Unfortunately, all attempts led to either cell death within 5 cell doublings or to at most ~50% reduction of expression, after which the expression was quickly reactivated to normal levels of the cells died (Fig. S3). This is in accordance with previous experiments in *D. melanogaster* [32], in *S. cerevisiae* and in mammalian model systems [25–27]. Bioinformatic analysis of a large number of cell lines in which PSMD14 was knocked out indeed indicates that PSMD14 is an essential gene for cell functioning (Fig. 1E) [54,55].

We then set out to further characterize the cell lines in which USP14 and UCH37 activity was strongly reduced or absent. Since both USP14 and UCH37 have DUB activity, the modulation of their expression levels is expected to perturb the cellular ubiquitinome, which is defined as the total complement of all ubiquitinated proteins in a cell at a given time point. Visual inspection of immunoblots of cell extracts probing for ubiquitin revealed no significant changes in the overall abundance of ubiquitinated proteins upon depletion of USP14 and UCH37 (Figs. 2 A, B). In contrast, WT cells that were treated with the proteasome inhibitor Bortezomib (Btz) for 8 h showed a massive upregulation of (poly)ubiquitination of proteins as indicated by the darker staining in the higher molecular weight region of the SDS-PAGE gel. Also, no differences in ubiquitination status between the KD or KO cells was observed. We therefore hypothesize that if the ubiquitination status of proteins or specific subsets of proteins, would be affected, then these modulations are likely more subtle and should be studied by more advanced tools.

Next, we investigated the stability of the multi-subunit proteasome upon depletion of UCH37 and USP14 using glycerol density ultracentrifugation combined with immunoblotting. By loading samples onto a 5–30% glycerol gradient and spin them at high gravity values, protein assemblies are distributed through the gradient according to their size. Larger structures will be clustered in the denser glycerol fractions, whereas smaller complexes and non-complexed proteins will end up in the less dense fractions. The distribution of the 20S proteasomal subunit PSMA5 suggests that the bulk of the protein is present in large complexes, most likely as an integral part the 20S and/or 26S proteasomes (Fig. 2C). In contrast, the distribution of both UCH37 and USP14 in WT cells was not limited to the fractions in which PSMA5 was located. These results suggest that relatively large fractions of USP14 and UCH37 in the cell are not associated to the proteasome and are in agreement with previous results published by the DeMartino lab [56]. In dKO cells, but not in single UCH37 or USP14 knockout cells, the distribution of PSMD14 is shifted to lower glycerol percentage fractions, indicating that PSMD14 is present in smaller structural entities. This might be caused by a decreased stability of the 19S proteasome, induced by the absence of UCH37 and USP14. It has been shown previously that USP14, besides a catalytic activity, also provides structural stability in the proteasome [30,57], so its depletion may affect the overall structure of the proteasome.

Tubulin was first used as a loading control to equalize total protein input amounts, but then unexpectedly showed a differential distribution pattern in the investigated cell lines. The distribution of tubulin was clearly downshifted to smaller structures as a result of depletion of USP14, UCH37 or both simultaneously. In fact, this result triggered us to investigate potential differences in the cytoskeleton structure in these cell lines. Depletion of UCH37 and USP14 simultaneously resulted in cellular morphology differences and a lower degree of intercellular contacts than WT cells, as observed by light microscopy. The localization of actin filaments was visualized using a fluorescent phalloidin analog that binds to F-actin (Fig. 2D). Clearly, USP14KO and dKO cells, but not UCH37KO cells, showed more stress fibers, as indicated by the more intense staining and a markedly different morphology. The molecular mechanism of stress induction upon absence of USP14, which directly or indirectly results in morphology changes will be the subject of future studies.

One way to test proteasome activity is to monitor cell survival upon treatment with agents that induce the unfolded protein response (UPR), such as tunicamycin and dithiothreitol [58]. Cells in which USP14 and UCH37 are depleted were more sensitive to these stress inducing agents, albeit that the effect was only limited (Figs. 2F, G). This suggest that, while the proteasome is apparently still performing sufficiently
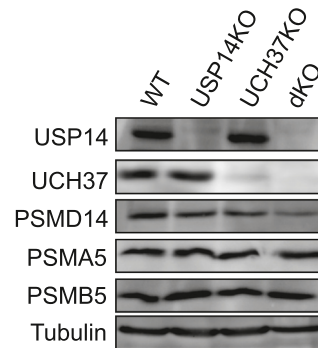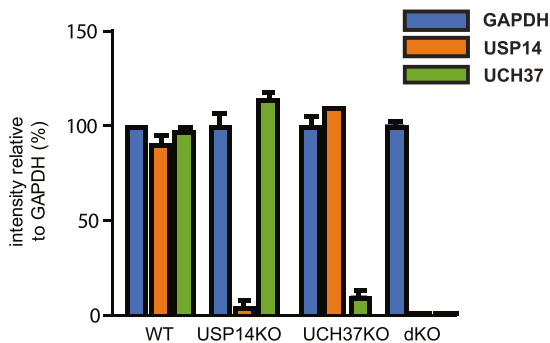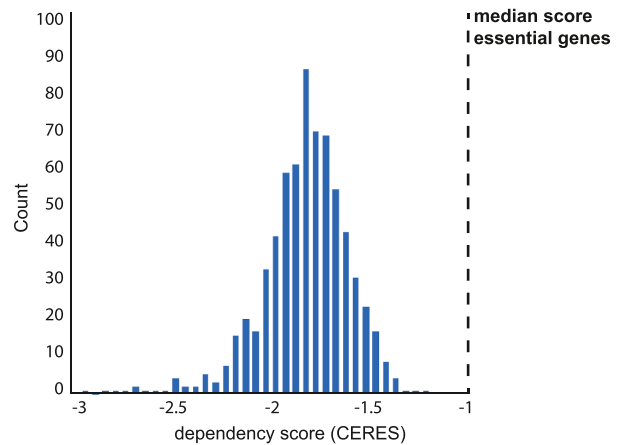
A)
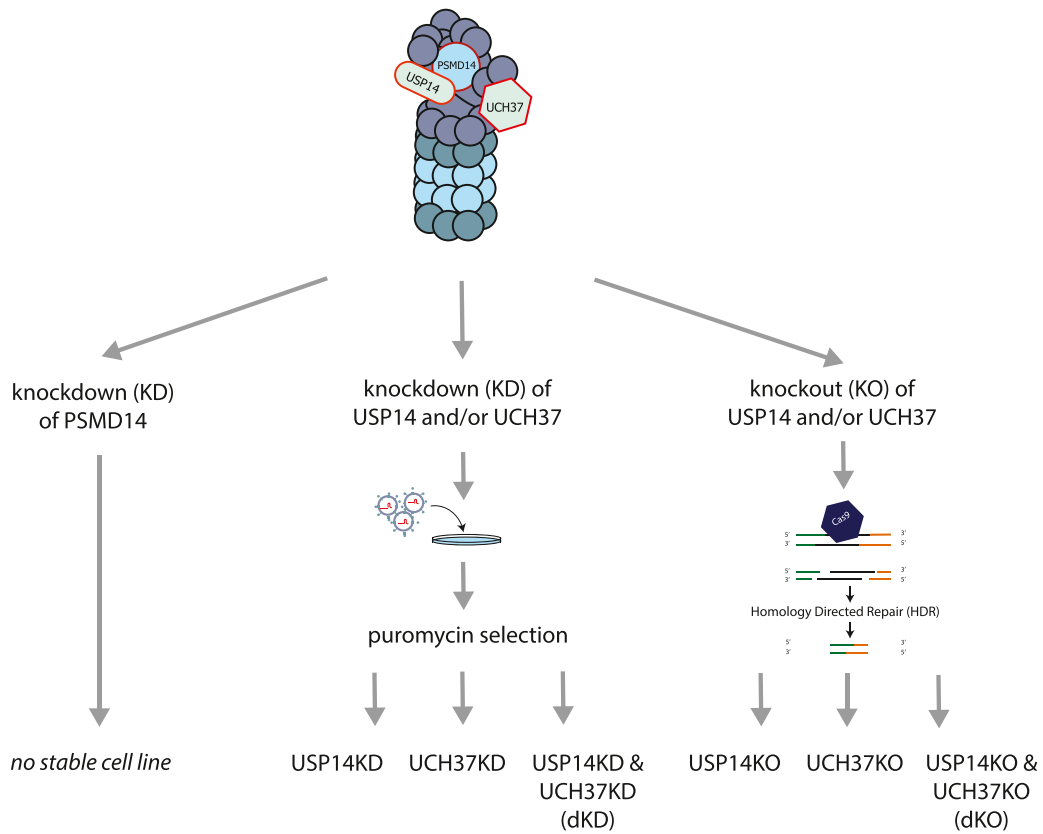
B)
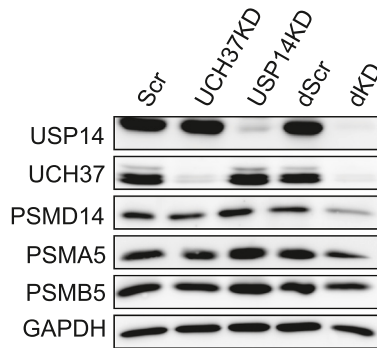
C)

D) Expression of proteasomal DUBS in KO cell lines

E) Dependency of PSMD14 in cell lines

(caption on next page)

Fig. 1. Construction and validation of knockdown (KD) and knockout (KO) cell lines for USP14, UCH37 and PSMD14. A) Scheme for the construction of cell lines. Knockdown cell lines were prepared using lentiviral shRNA, while knockout cell lines were constructed using CRISPR-Cas9. Attempts to reduce the expression of PSMD14 led to either incomplete reduction or cell death. Control cell lines for knockdown were transduced with one (Scr) or 2 (dScr) scrambled shRNAs. A visual representation of the location of the PAM sequences used to target USP14 and UCH37 is shown in Fig. S1. B, C) Cell lines were checked for expression of indicated proteins using immunoblotting. D) Relative expression levels of USP14, UCH37 and GAPDH (control) were measured using a targeted mass spectrometry parallel reaction monitoring (PRM) assay. For each of these proteins, multiple tryptic peptides were targeted and their intensities were averaged and compared. The intensity values were normalized to expression levels of GAPDH, which was then set at 100% for all cell lines. See Fig. S2 for the PRM transitions of a representative target peptide. For both USP14 and UCH37, no expression at all was detected in the dKO cell line. E) Histogram of viability scores of 651 cell lines with PSMD14 knocked out using CRISPR-Cas9. The dependency was scored using CERES scoring, where 0 is non-essential and − 1 is the median of essential genes. With a median score of- 1.9, PSMD14 was deemed essential. Input data were from https://depmap.org/portal/.

adequately to maintain a steady state of cell survival, loss of the two DUBs seems to lead to a higher level of sensitivity towards cellular stress, possibly related to a reduced ubiquitin editing proficiency. In addition, depletion of either USP14 or UCH37 seemed already sufficient to sensitize cells to stress inducing agents, with loss of USP14 showing the strongest effect.

Next, we sought to investigate putative differences in the interactomes of proteasomes in WT cells versus cells in which USP14 and UCH37 were depleted. We hypothesized that there may be yet unknown proteins stably or loosely associated to the proteasome that could play a direct or indirect role in the ubiquitin chain trimming mechanism by USP14 and UCH37. To test this, intact proteasomes of WT cells and dKO cells were immunopurified and a label-free quantification mass spectrometry strategy was applied to determine putatively differential interacting partners (Figs. 2E, S4). We identified several putative interactors specific to WT proteasomes that were not identified in the interactome of proteasomes depleted for USP14 and UCH37, such as the ubiquitin ligase UBE3C. Although we currently have no further evidence for this, it is tempting to speculate about the occurrence of specific E3 ligase / DUB pairs. The involvement of several of the interacting proteins will be the subject of further studies. Other proteins interacting exclusively with WT proteasomes include the multitasking protein SET, creatine kinase B-type, the transcriptional coactivator flightless homolog, the ribosomal protein Rps23 (but no additional ribosomal factors) and the metabolic enzyme malate dehydrogenase. All identified proteins are listed in Table S1–3.

Although several hypotheses have been postulated in the literature, it is still largely unknown why the proteasome contains three subunits with apparent overlapping DUB functionalities. While PSMD14 seems to be essential for the proteasome, there may be some redundancy between UCH37 and USP14 [25,56,59]. Inhibition studies have shown that loss of USP14 activity leads to a hyperactive proteasome [57]. Still, there have been no studies to date that have identified specific targets for these proteasomal DUBs. To investigate whether UCH37 or USP14 targets specific protein substrates or perhaps specific ubiquitin linkage types, we applied a proteomics based assay to compare the composition of the global proteome and ubiquitinome in WT cells and in cells depleted for both DUBs. Such an in-depth quantitative ubiquitination site analysis may give insights into the functions of these DUBs. We set up a SILAC mass spectrometry approach in which WT or (d)KD/(d)KO cells were grown in medium containing isotopically labeled lysine and arginine in an experimental duplicate label swap configuration (Fig. 3A). For the global ubiquitinome analysis, enrichment of ubiquitinated sites by immunopurification of diGly peptides was performed prior to mass spectrometry analysis (Fig. 3A, Table 1).

First, cells in which the DUBs were knocked out rather than knocked down showed a similar perturbation of the ubiquitinome (Fig. 4A), although the perturbation of the global proteome was more pronounced in the dKO cell line (Fig. 3B). In addition, the loss of both proteasomal DUBs simultaneously resulted in a more pronounced modulation of the ubiquitinome compared to the loss of only one proteasomal DUB at a time both in the KD and the KO cell lines, which would be in agreement with the alleged redundant roles for UCH37 and USP14 [23]. On the other hand, if the DUBs would be functionally redundant, the single KD and KO cells would show and only very limited or no modulation of the

ubiquitinome, as their respective counterparts would compensate for loss of DUB activity. In order to further test the redundancy hypothesis, we compared the up- and downregulated ubiquitination sites between the different depletion conditions to determine overlapping sites and/or target proteins (Fig. 4B–D). In these analyses, we also included ubiquitination sites that were consistently detected in the Light SILAC channel but completely absent in the Heavy channel or vice versa, and therefore have no reported H:L ratio in the MaxQuant output tables. Such diGly peptides are considered interesting target sites, since they represent ubiquitination sites that are induced or deleted as a result of the treatment, and as such may give information about the pathways affected by the loss of proteasomal DUBs. Surprisingly, the sets of up- and downregulated diGly peptides identified in duplicate experiments for every condition showed only limited overlap, with the vast majority of ubiquitination sites only detected in one or two of the cell lines studied (Fig. 4B–D). Also, there was an only limited overlap in proteins with differential ubiquitination status. We therefore set out to determine the overlap in functional categories of proteins with affected ubiquitylation status. Sets of differentially up- and downregulated diGly peptides *c.q.* ubiquitination sites were subjected to gene ontology analysis to search for affected pathways (Fig. 4E and Fig. S7). Since depletion of both USP14 and UCH37 simultaneously resulted in the strongest perturbation of the ubiquitinome, the number of differential ubiquitylation sites is high, resulting in a more pronounced GO analysis output. Amino acid sequence motif analysis of ubiquitination sites upregulated in the (d)KD and (d)KO cells did not reveal any consensus target sites in any of the diGly peptide data sets (Fig. S6), suggesting that USP14 and UCH37 do not target specific peptide sequences. However, we cannot exclude from these analyses that substrates of USP14 and/or UCH37 may be recognized based on target protein structure or on specific polyubiquitin linkage types.

We then interrogated the ubiquitinome data set to call for proteins with consistent, differential patterns of ubiquitylation status at multiple sites. In this analysis, diGly peptides were included for further analysis only if they were present in at least three out of four conditions. Three proteins (SQSTM1, RAD18 and PLXND1) with striking ubiquitylation patterns were selected to highlight the dynamics of the ubiquitylation patterns, which may also shed light on some of the phenotypic traits observed in cells depleted for the two proteasomal DUBs. SQSTM1 is a receptor for selective autophagy which was found to be extensively ubiquitinated upon depletion of both USP14 and UCH37 or UCH37 knockdown alone (Fig. 5A-B), while its abundance was upregulated only in UCH37KO cells (Table 2). Ubiquitination of K420 in SQSTM1 has been shown to induce autophagy [60] and SQSTM1 may permit the cell to use autophagy to compensate for proteasomes that have impaired ubiquitin recognition or (editing) DUB activity [61]. Possibly, the induction of autophagy by SQSTM1 ubiquitination could be a compensatory mechanism for the affected proteasome functionality due to decreased DUB activity without leading to cell death. In cells in which only USP14 was depleted no upregulation of ubiquitination was observed, in contrast to UCH37KD/KO and dKD/dKO cells. Possibly, since the loss of USP14 results in a hyperactive proteasome [30,57], the lack of ubiquitylation of SQSTM1 after loss of USP14 indicates that the cell does not need to turn to autophagy to degrade proteins.

The E3 ligase RAD18 ubiquitinates PCNA in UV induced DNA
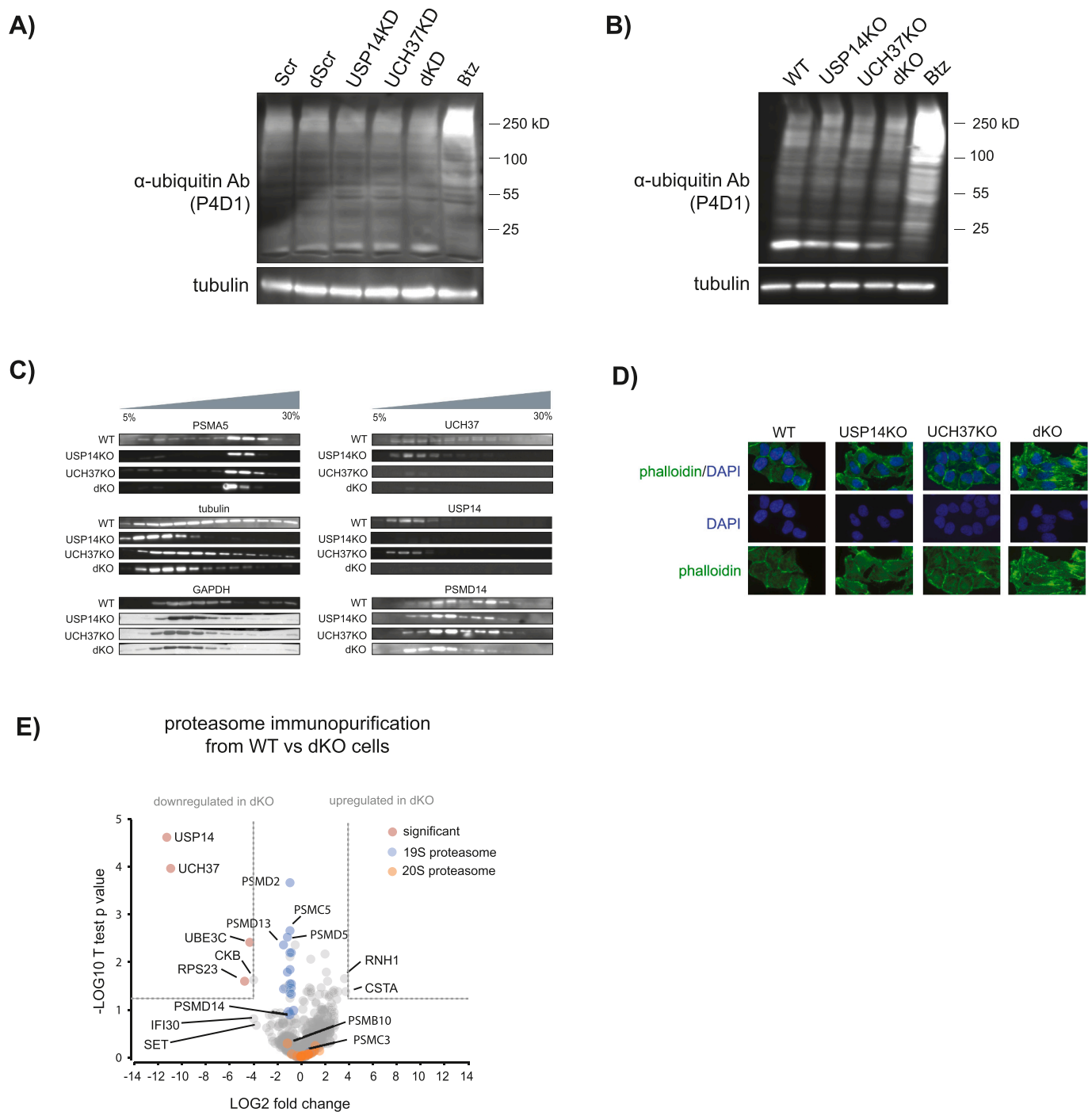
Fig. 2. Characterization of knockdown and knockout cell lines. A, B) Ubiquitinated proteins were visualized by immunoblotting with an antibody against ubiquitin (P4D1) for both KD cells (A) and KO cells (B). The positive control is an extract of WT cells that were treated with Bortezomib for 8 h. C) Glycerol gradient sedimentation assay to inspect the integrity of the proteasome under different conditions. The presence of proteins in either the lower density glycerol fractions (left side) or the higher density glycerol fractions (right side) indicates whether they are part of smaller or larger protein assemblies, respectively. Proteins were visualized by immunoblotting with the indicated antibodies, GAPDH served as a loading control. D) Immunofluorescence staining of F-actin using phalloidin for the indicated cell lines. E) Comparison of affinity-purified (AP) proteasomes using the Ubl domain of RAD23 in WT cells and dKO cells and analyzed by label free quantification (LFQ) mass spectrometry. All AP-MS assays were performed in triplicate. Blue data points indicate 19S proteasome subunits, orange data point indicate 20S proteasome subunits and red data points represent significantly altered ratios. A fold change (LOG2) of 4 was taken as a cut off value (see Table S1-S3 for MS data).

damage repair [62]. The ubiquitination status of RAD18 controls its interactions and functions. In undamaged cells, RAD18 exists in equilibrium between the ubiquitinated and non-ubiquitinated state and forms complexes with distinct binding partners. However, upon DNA damage Rad18 becomes deubiquitinated [63]. In our assay, RAD18 displays a striking increase in ubiquitination status at multiple target lysine residues, most notably in cells depleted for USP14 and UCH37 (Fig. 5A). Also, the observed slower growth of dKO cells compared to WT cells could be explained by a possibly less effective DNA damage repair system in these cells. Additional functional experiments are needed to further investigate the ubiquitination dynamics of RAD18.

PLXND1 is a cell surface protein that can bind several semaphorins
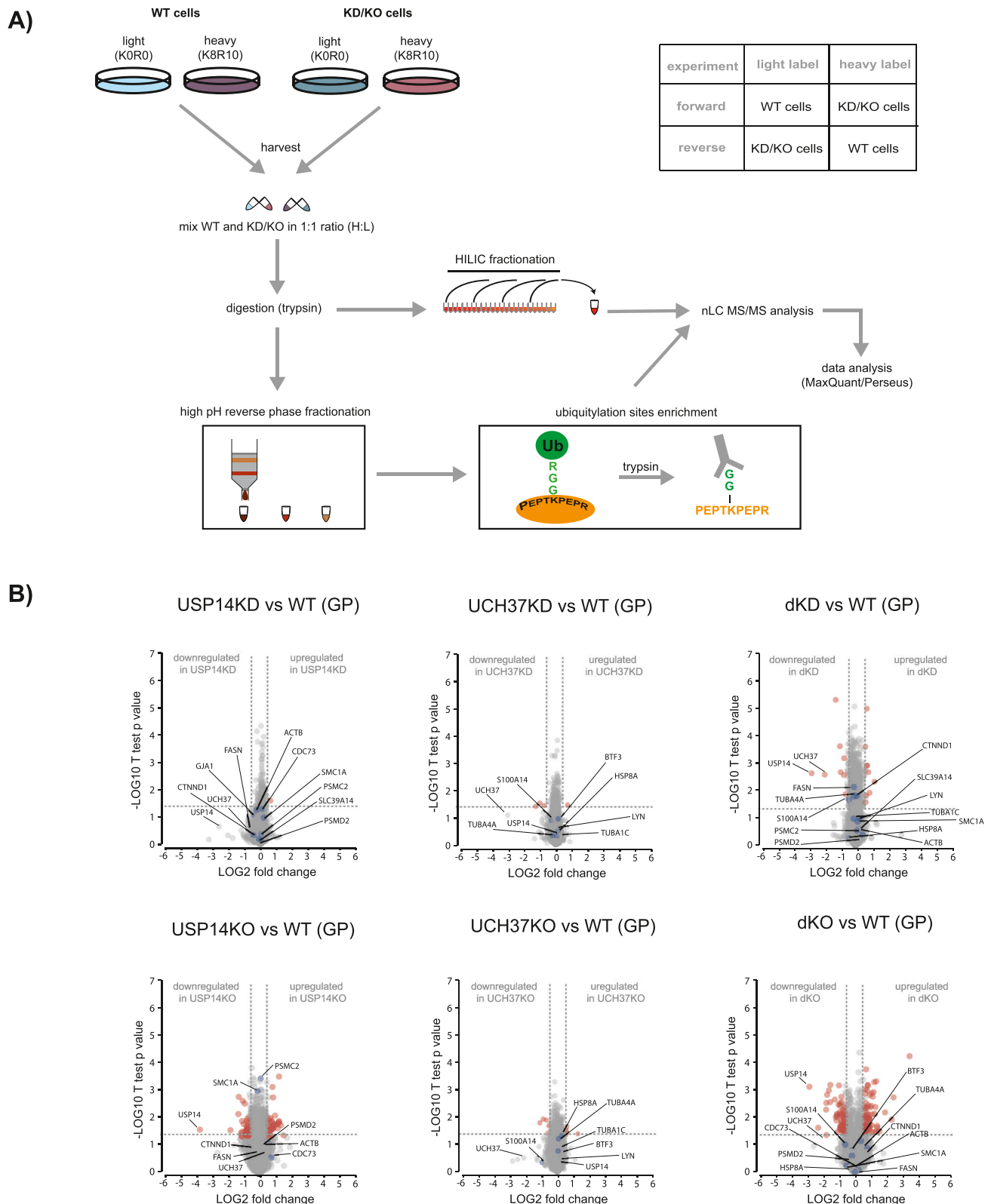
Fig. 3. A) SILAC mass spectrometry workflow for the quantitative comparison of the global proteomes and ubiquitinome of knockdown and knockout versus WT cell lines. For the ubiquitinome analyses, diGly peptides were enriched for using immunopurification with an anti-K-ε-GG antibody (CST). All SILAC experiments were performed in a forward (FW) and reverse (RV) configuration based on heavy isotope label swapping. B) Volcano plots showing the LOG2 fold changes and corresponding *p*-values from *t*-test analyses for in total 7557 proteins and thus indicate the changes in the global proteomes of indicated cell lines. For all analyses an (arbitrary) cut-off value of 1.5-fold up- or downregulation was taken as the threshold. Blue data points represent proteins in which diGly sites are significantly up- or downregulated in at least 4 out of 6 conditions (see Fig. 4).

Table 1

All identified and quantified diGly peptides.

diGly peptides	Total	Total FW	Total RV	Up FW	Up RV	Up FW + RV	Down FW	Down RV	Down FW + RV
USP14KD	12,398	10,424	8231	716	270	24	801	716	77
UCH37KD	9954	8438	5738	615	430	15	1537	307	52
USP14KD + UCH37KD	12,576	10,466	10,049	439	898	112	1867	1363	632
USP14KO	4845	3352	2504	346	320	56	548	288	90
UCH37KO	4777	3828	3585	331	471	104	368	464	143
USP14KO + UCH37KO	11,888	6097	5441	837	850	185	3037	686	241
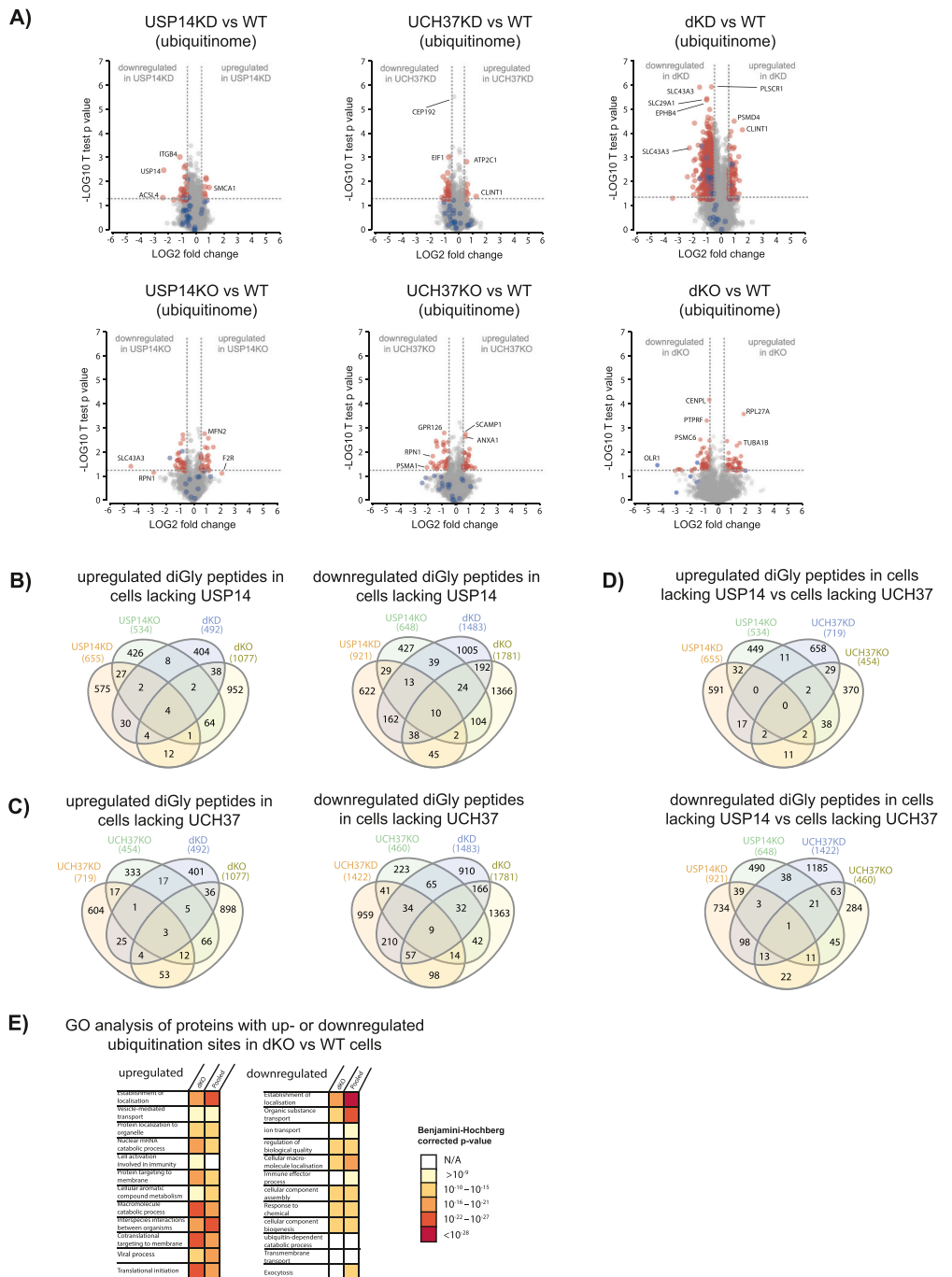
Fig. 4. A) SILAC mass spectrometry ubiquitinome analysis of cells in which UCH37 and/or USP14 were depleted. The volcano plots show the LOG2 fold changes of each identified diGly peptide. The dotted lines represent the (arbitrary) cut-off values of 1.5-fold up- or downregulation and p-value <0.05. Blue data points represent diGly peptides of which the associated proteins are described in detail in Fig. 5. See Table 1 for all details about the identified and quantified diGly peptides detected in distinct conditions and Table S4 for an overview of detected ubiquitination sites that were correlated with global protein expression. B–D) Overlap of identified diGly peptides in cells in which UCH37 and/or USP14 were depleted. Both up- and downregulated sites were compared for overlap to determine putative protein targets of UCH37 and USP14 DUB activity. E) Gene ontology (GO) analysis using Gorilla revealed that proteins in which ubiquitination sites were differentially regulated between WT and KD/KO cells are involved in processes including macromolecule catabolic processes and establishment of localization. See Fig. S7 for a more detailed overview.

and has been implicated in migration of T-cells and as a mechanosensory protein in endothelial cells, among other functions [64]. In cells lacking USP14 and/or UCH37, a strong decrease in ubiquitylation was observed in the intracellular RasGAP domain, which is important for transmission of the extracellular signal to the interior of the cell. Since the morphology of USP14KO cells is rather different from those of WT and UCH37KO cells (Fig. 2D), the decrease of PLXND1 ubiquitylation might be associated with a phenotype with affected motility, perhaps reducing
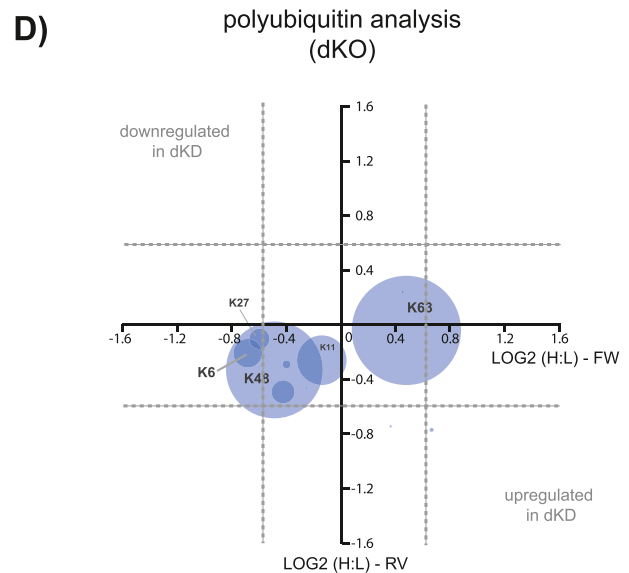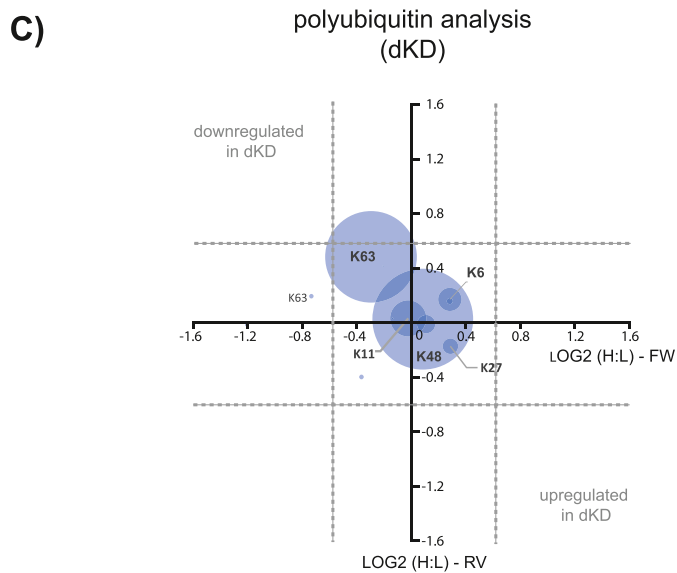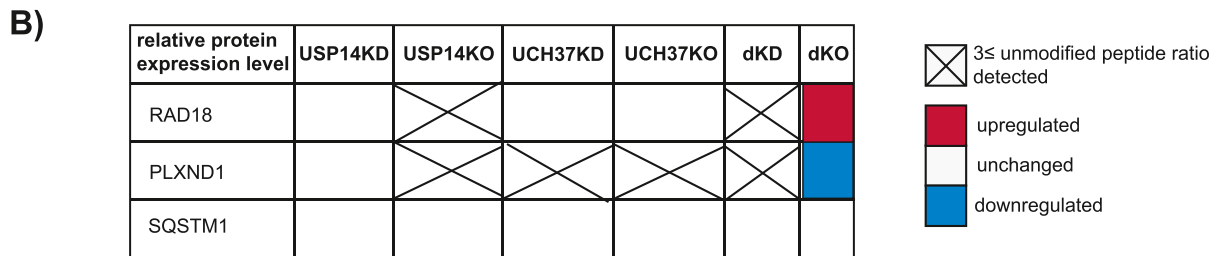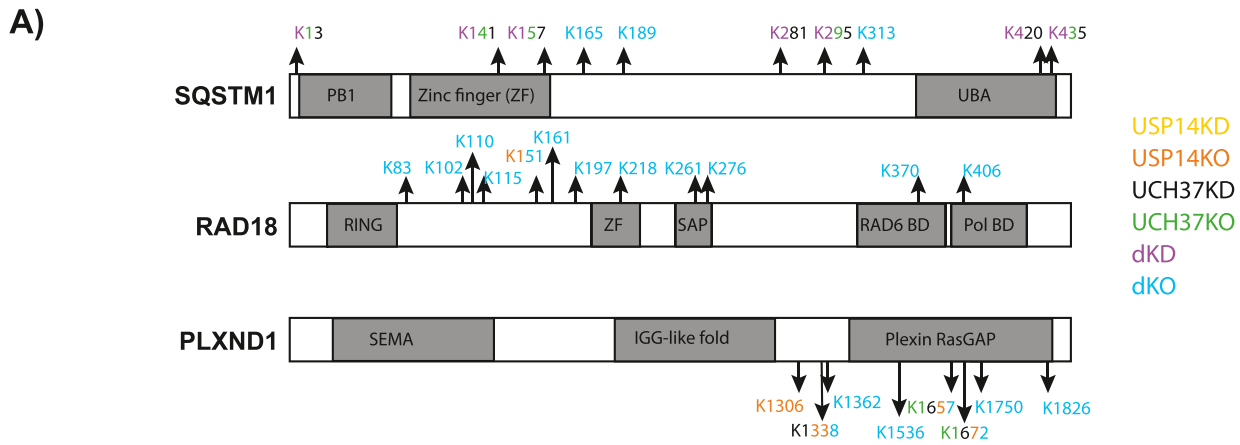
Fig. 5. A) Selection of several proteins whose ubiquitination profiles were differentially regulated as a result of UCH37 and/or USP14 depletion. The direction of the arrow indicates whether the ubiquitination site is up- or downregulated, while the color of the indicated lysine residue indicates the experimental condition. Up- or downregulation was arbitrarily defined as >1.5-fold abundance changes as determined from SILAC ratios. Lysine residues in multiple color print indicate that abundance changes were observed under multiple experimental conditions. B) Changes in the global expression levels of the selected target proteins in panel A). See also Table 2. C, D) Comparative analysis of polyubiquitin linkage types. The modified lysine residues of ubiquitin tryptic peptides are indicated for the prominent data points representing ubiquitin diGly peptides. Data points in the upper left quadrant represent ubiquitin diGly peptides which were downregulated in dKD / dKO cells, while data points in the lower right quadrants represent peptides that were upregulated in the respective conditions. The size of the data points reflects the relative spectral intensity of the respective peptides. Data for the single KD and KO experiments are shown in Fig. S5.

Table 2
Fold change of proteins described in Fig. 5A and B.

	USP14KD	USP14KO	UCH37KD	UCH37KO	DKD	DKO
Protein	Fold change (Log2)	Fold change (Log2)	Fold change (Log2)	Fold change (Log2)	Fold change (Log2)	Fold change (Log2)
RAD18	−0.03	ND	0.18	0.39	ND	0.73
PLXND1	0.02	ND	ND	ND	ND	−1.11
SQSTM1	−0.06	−0.05	0.12	0.45	0.00	0.14

the adherent strength by which the cells attach to the tissue culture dish.

To investigate whether USP14 and UCH37 have different ubiquitin linkage target specificities, we scrutinized the ubiquitin specific tryptic diGly peptides in (d)KD and (d)KO cells. Although diGly peptides representing all possible polyubiquitin linkage types could be identified (albeit in varying abundances), the differences between WT and (d)KD/(d)KO cells were only subtle (Fig. 5C–D). In KD cells a small downregulation of K63 linkages could be observed, whereas in the KO cells the small differences were not consistent between the duplicate swap experiments and are therefore inconclusive. Clearly, no obvious specific target specificity for UCH37 and/or USP14 could be assessed with respect to poly-ubiquitin linkage type. The alleged functional redundancy between USP14 and UCH37 was not reflected in specific ubiquitin linkage targeting either. As expected, in the single KD and single KO cell lines, we did not observe any significant differences in specific polyubiquitin linkage types either (Fig. S5).

Next, we investigated how the depletion of the proteasomal DUBs would affect the sensitivity of cells to chemical modulation of the proteasome by using specific inhibitors. Upon incubating cells with Bortezomib, which inhibits proteasomal activity by targeting the chymotrypsin-like activity of the β5 subunit [7], dKO cells seemed to be more sensitive in a crystal violet-staining survival assay compared to WT cells (Fig. S8). However, upon treatment of cells with the small molecule compound b-AP15, which was reported to specifically target both UCH37 and USP14 [65], no differential effect was observed (Fig. S8). This was unexpected, because dKO cells lack both of the supposed specific b-AP15 targets and hence are expected to be not or much less susceptible to the compound than WT cells, unless it has - yet unknown – off-target effects. In order to test the effect of small molecule compounds that intervene with proteasome DUB activity in more detail, the global ubiquitinomes of WT and dKO cells treated with b-AP15 or mock treated were compared. In general, a strong upregulation of ubiquitination events was observed upon treatment of both WT and dKO cells with b-AP15 (Fig. 6B–D). GO analysis revealed that the majority of the pathways involved were overlapping between the two cell lines (Fig. 6E, F).

The above results strongly suggest that b-AP15 has off-target effects, besides the reported exclusive activity directed towards USP14 and UCH37, which interfere with other elements of the UPS. To test which additional proteins, apart from USP14 and UCH37, are targeted, WT versus dKO cells treated with b-AP15 were directly compared (Fig. 7). Dynamic ubiquitinome analyses to assess the effect of USP14 and UCH37 knockdown in a b-AP15 treatment background revealed that there is a substantial set of differential diGly peptides that are either specifically upregulated in the dKO cells or in the WT cells (Fig. 7A, B). In addition, we did not observe any major differences in the relative abundances of diGly peptides representing different polyubiquitin linkage types in the comparison between WT and dKO cells treated with b-AP15, although K63 appears to be slightly downregulated in dKO cells as opposed to K48 (Fig. 7C).

The results of the separate (Fig. 6) and combined (Fig. 7) assays are in agreement in that the treatment of dKO cells with b-AP15, in which its alleged targets are depleted for, results in an even more pronounced remodeling of the ubiquitinome than in WT cells treated with b-AP15. If b-AP15 would exclusively target UCH37 and USP14, the effects on the ubiquitinome would be similar to the effects observed in the dKO cells, in which the activity of the two targets is absent. In that case, treatment

of WT cells or dKO cells with b-AP15 should make no difference, since in both conditions the activities of UCH37 and USP14 are completely abolished. In conclusion, these results show that b-AP15 has severe, yet unreported off-target effects that most likely involve the modulation of proteasome activity.

4. Discussion

In order to define the functional roles of the three different DUBs associated with the proteasome we applied a proteome and ubiquitinome analysis in cells with and without the endogenous expression of these DUBs, individually or in a combined fashion. Cells without PSMD14/RPN11 were not viable and this DUB was therefore excluded from further analysis. In total, we identified 56,436 diGly peptides, of which 21,458 were unique, representing in total 20,533 distinct ubiquitination sites. Such a level of ubiquitinome deepness suggests that *if* differential protein targeting specificities for these DUBs were to be expected, the sensitivity of the assay should be sufficiently high to detect those.

Surprisingly, the overlap between the identified differential diGly peptide populations in the USP14, UCH37 KD/KO and double KD/KO cells was only modest. This suggests that the targeting specificities for these DUBs may not overlap to a great extent, although previous studies have suggested that there is functional redundancy [57]. In case UCH37 and USP14 would be functionally redundant, the single KD/KO cells would show only limited modulation of the ubiquitinome, as their respective counterparts would compensate for loss of DUB activity. In contrast, the USP14/UCH37 double KD/KO cells are expected to show up- and downregulated diGly peptides, since if both UCH37 and USP14 activities are abolished they cannot be compensated for by their respective counterparts. Although we did observe overall higher numbers of regulated diGly peptides in the double KD/KO cells, the numbers of regulated diGly peptides in the single KD/KO cells were quite substantial. The high numbers of downregulated ubiquitination sites upon removal of DUB activity suggest regulatory roles for UCH37 and USP14. In proteasome inhibition experiments we have noticed that the far majority of ubiquitination sites are upregulated (and only few sites are downregulated) as a result of the accumulation of ubiquitinated proteins [44]. Also, the overlap between the single KD/KO cells and the double KD/KO cells is only limited, even though the latter obviously include the same target protein targeted in the first. This suggests that different populations of ubiquitination sites are targeted in the single versus the double KD/KO's, which would not be in disagreement with the redundancy theory. Finally, we cannot exclude the possibility that the lack of overlap in ubiquitination sites may be caused by the (widely applied) methodology to screen global ubiquitinomes, which may still capture only a subpopulation of the total ubiquitinome. Overall, the data set presented here is inconclusive when it comes to the assessment of redundancy level between UCH37 and USP14.

Next, we hypothesized whether USP14 and UCH37 could have differential targeting specificities for polyubiquitin linkage types. For this, we performed both global proteome and ubiquitinome screens and focused on ubiquitination sites on polyubiquitin itself. Most polyubiquitin specific ubiquitination sites appeared not to be differentially regulated upon depletion of either DUB or both simultaneously, suggesting that the DUBs do not target specific polyubiquitin linkage types either. However, we cannot exclude the possibility that potential
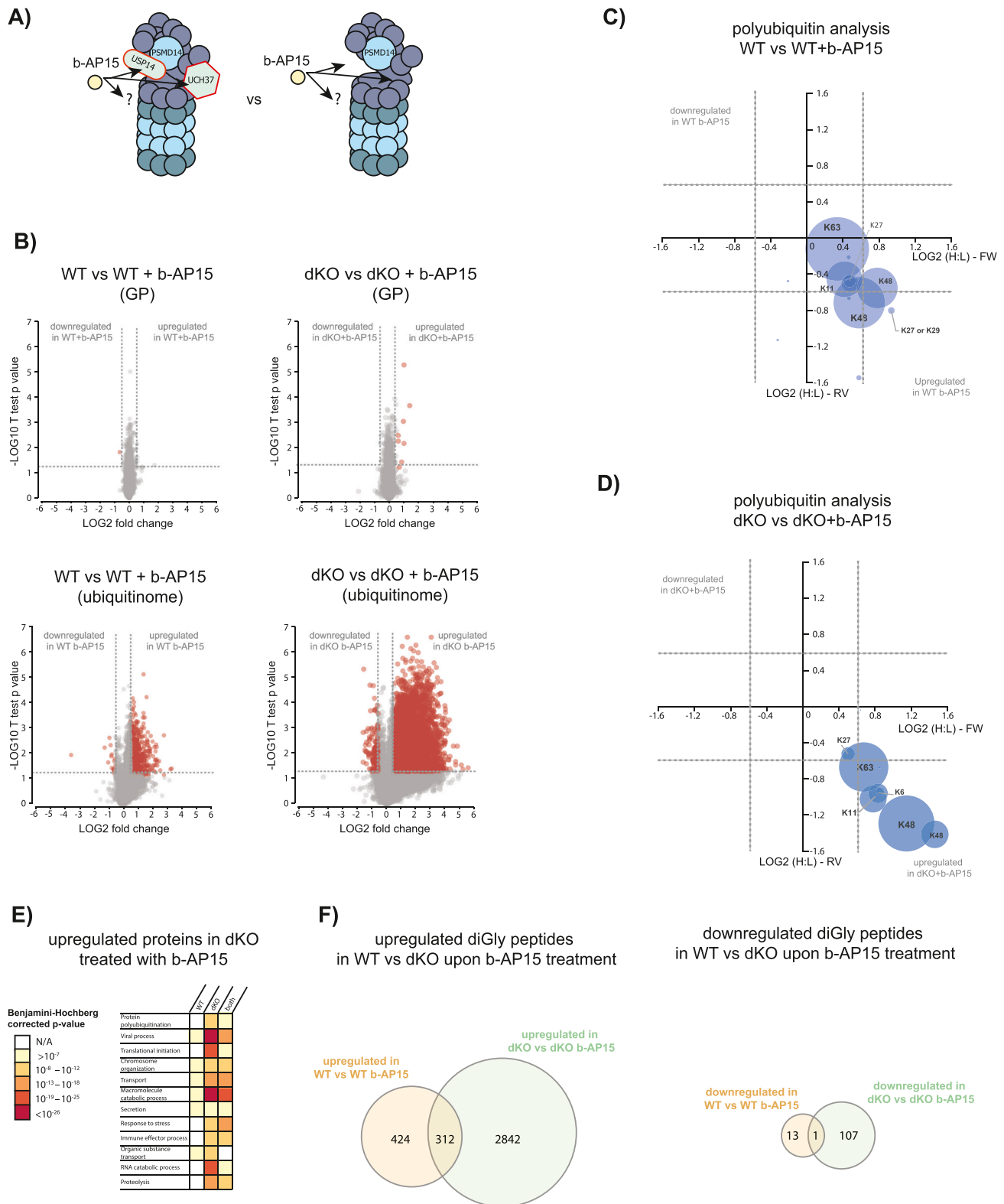
Fig. 6. Treatment of dKO cells with the small molecule inhibitor b-AP15 led to additional effects beyond the inhibition of UCH37 and USP14. A) Cartoon illustrating the hypothesis that b-AP15 may target other components in addition to UCH37 and USP14. B) Global proteome and ubiquitinome dynamics analysis of WT versus dKO cells treated with b-AP15 for 8 h suggests that the inhibitor b-AP15 strongly affects the global ubiquitinome and that the targeting specificity goes beyond the DUBs UCH37 and USP14. For a complete list of affected proteins and their ubiquitination sites, see Tables S5-S8. C) Ubiquitination site analysis of ubiquitin specific peptides upon treatment of WT cells with b-AP15, suggesting that the overall ubiquitination is increased with a preference for the K48 Ub-linkage. D) Ubiquitination site analysis of ubiquitin specific peptides upon treatment of dKO cells with b-AP15, suggesting that the overall ubiquitination is increased with a preference for the K48 Ub-linkage and the involvement in proteasomal degradation. E) Gene ontology analysis of b-AP15 treatment: several GO terms are significantly upregulated in b-AP15 treated WT vs dKO cells, based on increased ubiquitination events (threshold cutoff >1.5-fold difference in SILAC ratios). F) Overlap between upregulated or downregulated diGly peptides of WT and dKO cells treated with b-AP15.
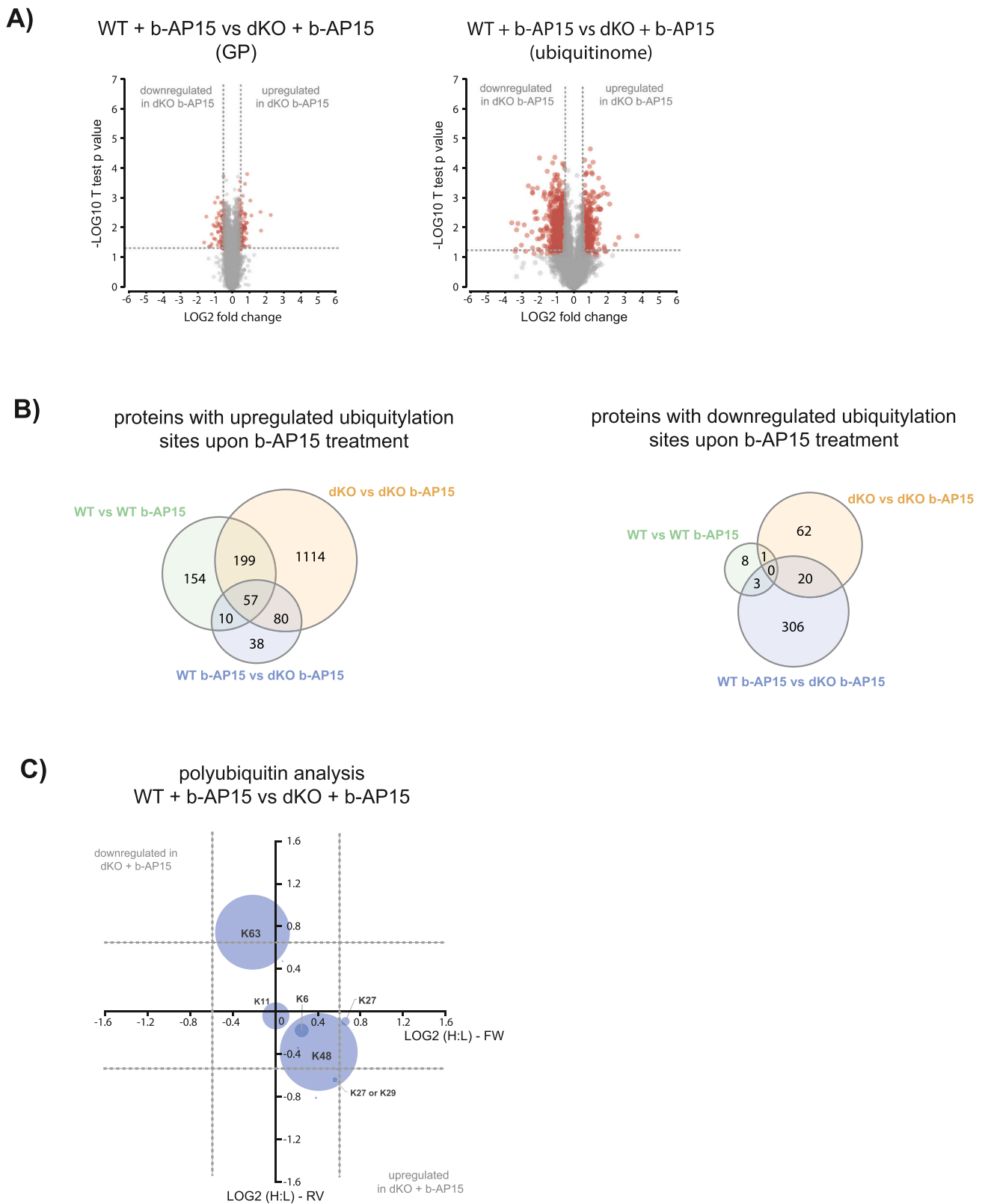
Fig. 7. In-depth analysis of the effect of the small molecule inhibitor b-AP15 on the global proteome and the ubiquitinome of cells depleted for both USP14 and UCH37. A) Analysis of the global proteomes and ubiquitinomes of b-AP15 treated WT cells versus b-AP15 treated dKO cells (see Tables S9–10 for the complete global proteome and ubiquitinome data sets). B, C) The overlap between proteins with increased ubiquitination as a result of b-AP15 treatment under different conditions suggests that - at least in part - the same population of proteins was affected. D) Polyubiquitin linkage type analysis of WT vs dKO cells that were both treated with b-AP15 for 8 h. Small but insignificant differences between the K63 linkage and the K48 linkage types were observed.

differential effects may be obscured by the presence of the total cellular ubiquitinome that is not affected by the action of these DUBs.

Recent work by Strieter et al. demonstrated that UCH37 can specifically target branched chains containing K48 linkages [42]. Although we did not observe a specific effect on K48 linkages in the UCH37 KO and/ or in UCH37 KD conditions, it should be noted that by analyzing diGly peptides upon tryptic digestion in a bottom-up approach all information on mixed linkage types is lost. Therefore, using the methodology described in this paper it is unfortunately not possible to distinguish between heterotypic and homotypic polyubiquitin chain branching. Middle- or top down mass spectrometry approaches could be useful for the determination of higher order polyubiquitin structures.

We have investigated the putative roles of USP14 and UCH37 in the unfolded protein response (UPR). Reduced proteasomal function may lead to accumulation of improperly folded proteins, which the cell is unable to remove or degrade. Induction of the UPR by treatment with tunicamycin or DTT showed a marked decrease in cell survival in cells in which either of the DUBs was knocked out as compared to wild type cells. This suggests that both in the single and double DUB knockout conditions cells have more difficulty in clearing improperly folded proteins, possibly as a result of impaired proteasome functioning. In contrast to previous results, these effects suggest the absence of redundancy between USP14 and UCH37.

In order to exclude unwanted side effects of the KD and KO depletion methods, USP14 and UCH37 were also inactivated by small molecule inhibitors. The inhibitor b-AP15 has been described to be specific for both DUBs [65]. However, upon treatment with b-AP15 the ubiquitinome was largely affected in dKO cells and to similar levels as in WT cells. The extensive modulation of the ubiquitinome in cells missing the two alleged targets of b-AP15 strongly suggests that the inhibitor targets additional cellular components besides USP14 and UCH37. In addition, affected ubiquitination sites in dKO cells treated with b-AP15 showed some overlap with affected sites in WT cells, indicating that there are common protein targets. Most likely, these substantial off-target effects of b-AP15 are directed towards the UPS, since the extent of upregulation of ubiquitination sites is extensive and comparable to the effects of e.g. the proteasome inhibitor Bortezomib [44]. The observation that b-AP15 targets additional cellular components besides USP14 and UCH37 raises questions to the alleged specificity of the inhibitor and its role in studies of the proteasome.

We hypothesized that, since the loss of both USP14 and UCH37 is not lethal to cells, depletion may result in the recruitment of alternative DUBs to the proteasome. To investigate this, we immunopurified proteasomes under various conditions and identified differentially associated proteins. We did, however, not detect major differences in proteasome composition nor in the presence of known proteasome associated proteins. Thus, the recruitment of alternative DUBs to the proteasome to cope with the loss of USP14 and UCH37 seems unlikely.

To assess the roles of all proteasome associated DUBs, it would be advantageous to also monitor the effects on the ubiquitinome upon depletion PSMD14. Unfortunately, complete removal or even the introduction of point mutations to make catalytic mutants were found to be lethal to cells [23,27]. Alternatively, PSMD14 could selectively be inactivated by using the inhibitor Capzimin [66]. This would be an interesting follow-up study and is also useful to characterize differences in the modes of action between various proteasome inhibitors.

In conclusion, in-depth ubiquitinome profiling of cells depleted for the proteasome associated DUBs in UCH37 and USP14 in comparison to WT cells was used to assess their cellular functions. Treatment of WT cells and cells depleted for UCH37 and USP14 with b-AP15, a small molecule inhibitor that supposedly targets both USP14 and UCH37, was found to remodel the ubiquitinome extensively. Based on these results it is highly unlikely that b-AP15 targets only UCH37 and USP14 and the targeting specificity is much broader. Finally, in-depth global proteomics and ubiquitinomics are valuable additions to the toolbox for the screening of existing and novel proteasome targeting drugs, some of which have already proven to be useful in the treatment of cancers such as multiple myeloma.

Data availability

No

Appendix A. Supplementary data

Supplementary data to this article can be found online at https://doi.org/10.1016/j.jprot.2022.104592.

References

[1] A. Hershko, A. Ciechanover, The ubiquitin system, Annu. Rev. Biochem. 67 (1998) 425–479, https://doi.org/10.1146/annurev.biochem.67.1.425.

[2] A. Ciechanover, The ubiquitin-proteasome proteolytic pathway, Cell 79 (1994) 13–21, https://doi.org/10.1016/0092-8674(94)90396-4.

[3] G. Atkin, H. Paulson, Ubiquitin pathways in neurodegenerative disease, Front. Mol. Neurosci. 7 (2014) 1–17, https://doi.org/10.3389/fnmol.2014.00063.

[4] D. Komander, M. Rape, The ubiquitin code, Annu. Rev. Biochem. 81 (2012) 203–229, https://doi.org/10.1146/annurev-biochem-060310-170328.

[5] S. Bergink, S. Jentsch, Principles of ubiquitin and SUMO modifications in DNA repair, Nature 458 (2009) 461–467, https://doi.org/10.1038/nature07963; 10.1038/nature07963.

[6] K.D. Tew, Commentary "proteasome inhibitors: a novel class of potent and effective antitumor agents", Cancer Res. 76 (2016) 4916–4917, https://doi.org/10.1158/0008-5472.CAN-16-1974.

[7] R. Oerlemans, N.E. Franke, Y.G. Assaraf, J. Cloos, I. van Zantwijk, C.R. Berkers, G. L. Scheffer, K. Debipersad, K. Vojtekova, C. Lemos, J.W. van der Heijden, B. Ylstra, G.J. Peters, G.L. Kaspers, B.A.C. Dijkmans, R.J. Scheper, G. Jansen, Molecular basis of bortezomib resistance: proteasome subunit beta5 (PSMB5) gene mutation and overexpression of PSMB5 protein, Blood 112 (2008) 2489–2499, https://doi.org/10.1182/blood-2007-08-104950.

[8] Y. Leestemaker, A. de Jong, K.F. Witting, R. Penning, K. Schuurman, B. Rodenko, E. A. Zaal, B. van de Kooij, S. Laufer, A.J.R. Heck, J. Borst, W. Scheper, C.R. Berkers, H. Ovaa, Proteasome activation by small molecules, cell, Chem. Biol. (2017) 1–12, https://doi.org/10.1016/j.chembiol.2017.05.010.

[9] E. Kim, S. Park, J.H. Lee, J.H. Kim, M. Kang, M.J. Lee, E. Kim, S. Park, J.H. Lee, J. Y. Mun, W.H. Choi, Y. Yun, J. Lee, Dual function of USP14 Deubiquitinase in cellular proteasomal activity and Autophagic flux article dual function of USP14 Deubiquitinase in cellular proteasomal activity and Autophagic flux, Cell Rep. 24 (2018) 732–743, https://doi.org/10.1016/j.celrep.2018.06.058.

[10] M.J. Clague, S. Urbé, Ubiquitin: Same molecule, different degradation pathways, Cell 143 (2010) 682–685, https://doi.org/10.1016/j.cell.2010.11.012.

[11] R. Yau, M. Rape, The increasing complexity of the ubiquitin code, Nat. Cell Biol. 18 (2016) 579–586, https://doi.org/10.1038/ncb3358.

[12] L. Herhaus, I. Dikic, Expanding the ubiquitin code through post-translational modification, EMBO Rep. 16 (2015) 1071–1083, https://doi.org/10.15252/embr.201540891.

[13] K.N. Swatek, J.L. Usher, A.F. Kueck, C. Gladkova, T.E.T. Mevissen, J.N. Pruneda, T. Skern, D. Komander, Insights into ubiquitin chain architecture using Ub-clipping, Nature 572 (2019) 533–537, https://doi.org/10.1038/s41586-019-1482-y.

[14] M.E. French, C.F. Koehler, T. Hunter, Emerging functions of branched ubiquitin chains, Cell Discov. 7 (2021) 1–10, https://doi.org/10.1038/s41421-020-00237-y.

[15] K. Okatsu, F. Koyano, M. Kimura, H. Kosako, Y. Saeki, K. Tanaka, N. Matsuda, Phosphorylated ubiquitin chain is the genuine Parkin receptor, J. Cell Biol. 209 (2015) 111–128, https://doi.org/10.1083/jcb.201410050.

[16] A. Ordureau, S.A. Sarraf, D.M. Duda, J.M. Heo, M.P. Jedrychowski, V. O. Sviderskiy, J.L. Olszewski, J.T. Koerber, T. Xie, S.A. Beausoleil, J.A. Wells, S. P. Gygi, B.A. Schulman, J.W. Harper, Quantitative proteomics reveal a feedforward mechanism for mitochondrial PARKIN translocation and ubiquitin chain synthesis, Mol. Cell 56 (2014) 360–375, https://doi.org/10.1016/j.molcel.2014.09.007.

[17] M. Unno, T. Mizushima, Y. Morimoto, Y. Tomisugi, K. Tanaka, N. Yasuoka, T. Tsukihara, The structure of the mammalian 20S proteasome at 2.75 Å resolution, Structure 10 (2002) 609–618, https://doi.org/10.1016/S0969-2126(02)00748-7.

[18] S. Murata, Y. Takahama, M. Kasahara, K. Tanaka, The immunoproteasome and thymoproteasome: functions, evolution and human disease, Nat. Immunol. 19 (2018) 923–931, https://doi.org/10.1038/s41590-018-0186-z.

[19] K. Husnjak, S. Elsasser, N. Zhang, X. Chen, L. Randles, Y. Shi, K. Hofmann, K. J. Walters, D. Finley, I. Dikic, Proteasome subunit Rpn13 is a novel ubiquitin receptor, Nature 453 (2008) 481–488, https://doi.org/10.1038/nature06926.

[20] X. Huang, B. Luan, J. Wu, Y. Shi, An atomic structure of the human 26S proteasome, Nat. Struct. Mol. Biol. 23 (2016) 778–785, https://doi.org/10.1038/nsmb.3273.

[21] D. Finley, Recognition and processing of ubiquitin-protein conjugates by the proteasome, Annu. Rev. Biochem. 78 (2009) 477–513, https://doi.org/10.1146/annurev.biochem.78.081507.101607.

[22] A.H. de la Peña, E.A. Goodall, S.N. Gates, G.C. Lander, A. Martin, Substrate-engaged 26S proteasome structures reveal mechanisms for ATP-hydrolysis–driven translocation, Science 362 (2018) eaav0725, https://doi.org/10.1126/SCIENCE.AAV0725.

[23] S.A.H. de Poot, G. Tian, D. Finley, Meddling with fate: the proteasomal Deubiquitinating enzymes, J. Mol. Biol. 429 (2017) 3525–3545, https://doi.org/10.1016/J.JMB.2017.09.015.

[24] R. Verma, L. Aravind, R. Oania, W.H. McDonald, J.R. Yates, E.V. Koonin, R. J. Deshaies, J.R. Yates III, E.V. Koonin, R.J. Deshaies, Role of Rpn11 metalloprotease in deubiquitination and degradation by the 26S proteasome, Science 298 (2002) 611–615, https://doi.org/10.1126/science.1075898.

[25] M. Gallery, J.L. Blank, Y. Lin, J.A. Gutierrez, J.C. Pulido, D. Rappoli, S. Badola, M. Rolfe, K.J. Macbeth, The JAMM motif of human deubiquitinase Poh1 is essential for cell viability, Mol. Cancer Ther. 6 (2007) 262–268, https://doi.org/10.1158/1535-7163.MCT-06-0542.

[26] A. Guterman, M.H. Glickman, Complementary roles for Rpn11 and Ubp6 in Deubiquitination and proteolysis by the proteasome, J. Biol. Chem. 279 (2004) 1729–1738, https://doi.org/10.1074/jbc.M307050200.

[27] G.R. Pathare, I. Nagy, P. Sledz, D.J. Anderson, H.-J.J. Zhou, E. Pardon, J. Steyaert, F. Forster, A. Bracher, W. Baumeister, P. Śledź, D.J. Anderson, H.-J.J. Zhou, E. Pardon, J. Steyaert, F. Förster, A. Bracher, W. Baumeister, Crystal structure of the proteasomal deubiquitylation module Rpn8-Rpn11, Proc. Natl. Acad. Sci. U. S. A. 111 (2014) 2984–2989, https://doi.org/10.1073/pnas.1400546111.

[28] L.R. Butler, R.M. Densham, J. Jia, A.J. Garvin, H.R. Stone, V. Shah, D. Weekes, F. Festy, J. Beesley, J.R. Morris, The proteasomal de-ubiquitinating enzyme POH1 promotes the double-strand DNA break response, EMBO J. 31 (2012) 3918–3934, https://doi.org/10.1038/emboj.2012.232.

[29] S.M. Buckley, B. Aranda-Orgilles, A. Strikoudis, E. Apostolou, E. Loizou, K. Moran-Crusio, C.L. Farnsworth, A.A. Koller, R. Dasgupta, J.C. Silva, M. Stadtfeld, K. Hochedlinger, E.I. Chen, I. Aifantis, Regulation of Pluripotency and cellular reprogramming by the ubiquitin-proteasome system, Cell Stem Cell 11 (2012) 783–798, https://doi.org/10.1016/J.STEM.2012.09.011.

[30] H.T. Kim, A.L. Goldberg, The Deubiquitinating enzyme Usp14 Allosterically inhibits multiple proteasomal activities and ubiquitin-independent proteolysis, J. Biol. Chem. 23 (2017) 9830–9839, https://doi.org/10.1074/jbc.M116.763128.

[31] A. Aufderheide, F. Beck, F. Stengel, M. Hartwig, A. Schweitzer, G. Pfeifer, A. L. Goldberg, E. Sakata, W. Baumeister, F. Förster, Structural characterization of the interaction of Ubp6 with the 26S proteasome, Proc. Natl. Acad. Sci. 112 (2015) 201510449, https://doi.org/10.1073/pnas.1510449112.

[32] K.A. Sap, K. Bezstarosti, D.H.W.H. Dekkers, O. Voets, J.A.A. Demmers, Quantitative proteomics reveals extensive changes in the Ubiquitinome after perturbation of the proteasome by targeted dsRNA-mediated subunit knockdown in Drosophila, J. Proteome Res. 16 (2017) 2848–2862, https://doi.org/10.1021/acs.jproteome.7b00156.

[33] H. Jung, B.-G. Kim, W.H. Han, J.H. Lee, J.-Y. Cho, W.S. Park, M.M. Maurice, J.-K. Han, M.J. Lee, D. Finley, E.-H. Jho, Deubiquitination of Dishevelled by Usp14 is required for Wnt signaling, Oncogenesis 2 (2013) e64, https://doi.org/10.1038/oncsis.2013.28.

[34] F. Massa, R. Tammaro, M.A. Prado, M. Cesana, B.-H. Lee, D. Finley, B. Franco, M. Morleo, The deubiquitinating enzyme Usp14 controls ciliogenesis and hedgehog signaling, Hum. Mol. Genet. 28 (2019) 764–777, https://doi.org/10.1093/hmg/ddy380.

[35] R.T. Vander Linden, C.W. Hemmis, B. Schmitt, A. Ndoja, F.G. Whitby, H. Robinson, R.E. Cohen, T. Yao, C.P. Hill, Structural basis for the activation and inhibition of the UCH37 deubiquitylase, Mol. Cell 57 (2015) 901–911, https://doi.org/10.1016/j.molcel.2015.01.016.

[36] L. Randles, R.K. Anchoori, R.B.S. Roden, K.J. Walters, The proteasome ubiquitin receptor hrpn13 and its interacting deubiquitinating enzyme Uch37 are required for proper cell cycle progression, J. Biol. Chem. 291 (2016) 8773–8783, https://doi.org/10.1074/jbc.M115.694588.

[37] D.D. Sahtoe, W.J. van Dijk, F. El Oualid, R. Ekkebus, H. Ovaa, T.K. Sixma, Mechanism of UCH-L5 activation and inhibition by DEUBAD domains in RPN13 and INO80G, Mol. Cell 57 (2015) 887–900, https://doi.org/10.1016/J.MOLCEL.2014.12.039.

[38] M.J. Clague, S. Urbé, D. Komander, Breaking the chains: deubiquitylating enzyme specificity begets function, Nat. Rev. Mol. Cell Biol. 20 (2019) 338–352, https://doi.org/10.1038/s41580-019-0099-1.

[39] B.-H. Lee, Y. Lu, M.A. Prado, Y. Shi, G. Tian, S. Sun, S. Elsasser, S.P. Gygi, R. W. King, D. Finley, USP14 deubiquitinates proteasome-bound substrates that are ubiquitinated at multiple sites, Nature 532 (2016) 1–16, https://doi.org/10.1038/nature17433.

[40] M. Hu, P. Li, L. Song, P.D. Jeffrey, T.A. Chernova, K.D. Wilkinson, R.E. Cohen, Y. Shi, Structure and mechanisms of the proteasome-associated deubiquitinating enzyme USP14, EMBO J. 24 (2005) 3747–3756, https://doi.org/10.1038/SJ.EMBOJ.7600832.

[41] J. Hanna, N.A. Hathaway, Y. Tone, B. Crosas, S. Elsasser, D.S. Kirkpatrick, D. S. Leggett, S.P. Gygi, R.W. King, D. Finley, Deubiquitinating enzyme Ubp6 functions noncatalytically to delay proteasomal degradation, Cell 127 (2006) 99–111, https://doi.org/10.1016/j.cell.2006.07.038.

[42] K.K. Deol, S.O. Crowe, J. Du, H.A. Bisbee, R.G. Guenette, E.R. Strieter, Proteasome-bound UCH37/UCHL5 Debranches ubiquitin chains to promote degradation, Mol. Cell 80 (2020) 796–809.e9, https://doi.org/10.1016/j.molcel.2020.10.017.

[43] G. Vere, R. Kealy, B.M. Kessler, A. Pinto-Fernandez, Ubiquitomics: an overview and future, Biomolecules 10 (2020) 1–22, https://doi.org/10.3390/biom10101453.

[44] L. Van Der Wal, K. Bezstarosti, K.A. Sap, D.H.W.W. Dekkers, E. Rijkers, E. Mientjes, Y. Elgersma, J.A.A.A. Demmers, Improvement of ubiquitylation site detection by Orbitrap mass spectrometry, J. Proteome 172 (2018) 49–56, https://doi.org/10.1016/j.jprot.2017.10.014.

[45] T. Masuda, M. Tomita, Y. Ishihama, Phase transfer surfactant-aided trypsin digestion for membrane proteome analysis, J. Proteome Res. 7 (2008) 731–740, https://doi.org/10.1021/pr700658q.

[46] L. Naldini, U. Blömer, P. Gallay, D. Ory, R. Mulligan, F.H. Gage, I.M. Verma, D. Trono, In vivo gene delivery and stable transduction of nondividing cells by a lentiviral vector, Science 272 (1996) 263–267, https://doi.org/10.1126/science.272.5259.263.

[47] F.A. Ran, P.D. Hsu, J. Wright, V. Agarwala, D.A. Scott, F. Zhang, Genome engineering using the CRISPR-Cas9 system, Nat. Protoc. 8 (2013) 2281–2308, https://doi.org/10.1038/nprot.2013.143.

[48] K. Bezstarosti, M. Lamers, J. van Kampen, B. Haagmans, J. Demmers, Targeted proteomics as a tool to detect SARS-CoV-2 proteins in clinical specimens, PLoS One 16 (2021) e0259165, https://doi.org/10.1371/journal.pone.0259165.

[49] J. Cox, M. Mann, MaxQuant enables high peptide identification rates, individualized p.p.b.-range mass accuracies and proteome-wide protein quantification, Nat. Biotechnol. 26 (2008) 1367–1372, https://doi.org/10.1038/nbt.1511.

[50] B. MacLean, D.M. Tomazela, N. Shulman, M. Chambers, G.L. Finney, B. Frewen, R. Kern, D.L. Tabb, D.C. Liebler, M.J. MacCoss, Skyline: an open source document editor for creating and analyzing targeted proteomics experiments, Bioinformatics 26 (2010) 966–968, https://doi.org/10.1093/bioinformatics/btq054.

[51] E. Eden, D. Lipson, S. Yogev, Z. Yakhini, Discovering motifs in ranked lists of DNA sequences, PLoS Comput. Biol. 3 (2007) e39, https://doi.org/10.1371/journal.pcbi.0030039.

[52] E. Eden, R. Navon, I. Steinfeld, D. Lipson, Z. Yakhini, GOrilla: a tool for discovery and visualization of enriched GO terms in ranked gene lists, BMC Bioinformatics 10 (2009) 48, https://doi.org/10.1186/1471-2105-10-48.

[53] N. Colaert, K. Helsens, L. Martens, J. Vandekerckhove, K. Gevaert, Improved visualization of protein consensus sequences by iceLogo, Nat. Methods 6 (2009) 786–787, https://doi.org/10.1038/nmeth1109-786.

[54] J.M. Dempster, J. Rossen, M. Kazachkova, J. Pan, G. Kugener, D.E. Root, A. Tsherniak, Extracting biological insights from the project Achilles genome-scale CRISPR screens in Cancer cell lines, BioRxiv (2019), 720243, https://doi.org/10.1101/720243.

[55] R.M. Meyers, J.G. Bryan, J.M. McFarland, B.A. Weir, A.E. Sizemore, H. Xu, N. V. Dharia, P.G. Montgomery, G.S. Cowley, S. Pantel, A. Goodale, Y. Lee, L.D. Ali, G. Jiang, R. Lubonja, W.F. Harrington, M. Strickland, T. Wu, D.C. Hawes, V. A. Zhivich, M.R. Wyatt, Z. Kalani, J.J. Chang, M. Okamoto, K. Stegmaier, T. R. Golub, J.S. Boehm, F. Vazquez, D.E. Root, W.C. Hahn, A. Tsherniak, Computational correction of copy number effect improves specificity of CRISPR-Cas9 essentiality screens in cancer cells, Nat. Genet. 49 (2017) 1779–1784, https://doi.org/10.1038/ng.3984.

[56] E. Koulich, X. Li, G.N. Demartino, Relative structural and functional roles of multiple Deubiquitylating proteins associated with mammalian 26S proteasome, Mol. Biol. Cell 19 (2008) 1072–1082, https://doi.org/10.1091/mbc.E07.

[57] B.-H.H. Lee, M.J. Lee, S. Park, D.-C.C. Oh, S. Elsasser, P.-C.C. Chen, C. Gartner, N. Dimova, J. Hanna, S.P. Gygi, S.M. Wilson, R.W. King, D. Finley, Enhancement of proteasome activity by a small-molecule inhibitor of USP14, Nature 467 (2010) 179–184, https://doi.org/10.1038/nature09299.

[58] H. Jiang, J. Zou, H. Zhang, W. Fu, T. Zeng, H. Huang, F. Zhou, J. Hou, Unfolded protein response inducers tunicamycin and dithiothreitol promote myeloma cell differentiation mediated by XBP-1, Clin. Exp. Med. 15 (2013) 85–96, https://doi.org/10.1007/s10238-013-0269-y.

[59] J.Y. Shin, S. Muniyappan, N.N. Tran, H. Park, S.B. Lee, B.H. Lee, Deubiquitination reactions on the proteasome for proteasome versatility, Int. J. Mol. Sci. 21 (2020) 1–16, https://doi.org/10.3390/ijms21155312.

[60] Y. Lee, T.-F. Chou, S.K. Pittman, A.L. Keith, B. Razani, C.C. Weihl, Keap1/Cullin3 modulates p62/SQSTM1 activity via UBA domain Ubiquitination, Cell Rep. 19 (2017) 188–202, https://doi.org/10.1016/J.CELREP.2017.03.030.

[61] A. Demishtein, M. Fraiberg, D. Berko, B. Tirosh, Z. Elazar, A. Navon, SQSTM1/p62-mediated autophagy compensates for loss of proteasome polyubiquitin recruiting capacity, Autophagy 13 (2017) 1697–1708, https://doi.org/10.1080/15548627.2017.1356549.

[62] W. Zhang, Z. Qin, X. Zhang, W. Xiao, Roles of sequential ubiquitination of PCNA in DNA-damage tolerance, FEBS Lett. 585 (2011) 2786–2794, https://doi.org/10.1016/j.febslet.2011.04.044.

[63] M.K. Zeman, J.R. Lin, R. Freire, K.A. Cimprich, DNA damage-specific deubiquitination regulates Rad18 functions to suppress mutagenesis, J. Cell Biol. 206 (2014) 183–197, https://doi.org/10.1083/jcb.201311063.

[64] V. Mehta, K.-L. Pang, D. Rozbesky, K. Nather, A. Keen, D. Lachowski, Y. Kong, D. Karia, M. Ameismeier, J. Huang, Y. Fang, A. del Rio Hernandez, J.S. Reader, E. Y. Jones, E. Tzima, The guidance receptor plexin D1 is a mechanosensor in

endothelial cells, Nature 578 (2020) 1–6, https://doi.org/10.1038/s41586-020-1979-4.

[65] Z. Tian, P. D'Arcy, X. Wang, A. Ray, Y.T. Tai, Y. Hu, R.D. Carrasco, P. Richardson, S. Linder, D. Chauhan, K.C. Anderson, A novel small molecule inhibitor of deubiquitylating enzyme USP14 and UCHL5 induces apoptosis in multiple myeloma and overcomes bortezomib resistance, Blood 123 (2014) 706–716, https://doi.org/10.1182/blood-2013-05-500033.

[66] J. Li, T. Yakushi, F. Parlati, A.L. Mackinnon, C. Perez, Y. Ma, K.P. Carter, S. Colayco, G. Magnuson, B. Brown, K. Nguyen, S. Vasile, E. Suyama, L.H. Smith, E. Sergienko, A.B. Pinkerton, T.D.Y. Chung, A.E. Palmer, I. Pass, S. Hess, S. M. Cohen, R.J. Deshaies, Capzimin is a potent and specific inhibitor of proteasome isopeptidase Rpn11, Nat. Chem. Biol. 13 (2017) 486–493, https://doi.org/10.1038/nchembio.2326.